Cell Metabolism
Article

Molecular and Genetic Crosstalks between mTOR and ERRα Are Key Determinants of Rapamycin-Induced Nonalcoholic Fatty Liver

Cédric Chaveroux,[1] Lillian J. Eichner,[1,5] Catherine R. Dufour,[1,5] Aymen Shatnawi,[1] Arkady Khoutorsky,[1] Guillaume Bourque,[4] Nahum Sonenberg,[1,2] and Vincent Giguère[1,2,3,*]
[1]Rosalind and Morris Goodman Cancer Research Centre, McGill University, 1160 Pine Avenue West, Montréal, QC H3A 1A3, Canada
[2]Department of Biochemistry
[3]Department of Medicine and Oncology
[4]Department of Human Genetics
McGill University, Montréal, PQ H3G 1Y6, Canada
[5]These authors contributed equally to this work
*Correspondence: vincent.giguere@mcgill.ca
http://dx.doi.org/10.1016/j.cmet.2013.03.003

SUMMARY

mTOR and ERRα are key regulators of common metabolic processes, including lipid homeostasis. However, it is currently unknown whether these factors cooperate in the control of metabolism. ChIP-sequencing analyses of mouse liver reveal that mTOR occupies regulatory regions of genes on a genome-wide scale including enrichment at genes shared with ERRα that are involved in the TCA cycle and lipid biosynthesis. Genetic ablation of ERRα and rapamycin treatment, alone or in combination, alter the expression of these genes and induce the accumulation of TCA metabolites. As a consequence, both genetic and pharmacological inhibition of ERRα activity exacerbates hepatic hyperlipidemia observed in rapamycin-treated mice. We further show that mTOR regulates ERRα activity through ubiquitin-mediated degradation via transcriptional control of the ubiquitin-proteasome pathway. Our work expands the role of mTOR action in metabolism and highlights the existence of a potent mTOR/ERRα regulatory axis with significant clinical impact.

INTRODUCTION

The mammalian target of rapamycin (mTOR), a phosphatidylinositol 3 kinase (PI3K)-related serine/threonine kinase, plays a major role in cell growth, proliferation and survival, in part by controlling messenger RNA (mRNA) translation (Wullschleger et al., 2006). mTOR is the core component of two distinct complexes: mTORC1 (complex 1) and mTORC2 (complex 2). mTORC1 is considered to be a central integrator of a wide range of physiological cues such as amino acid levels, energy status, and oxygen levels in order to promote cellular growth and proliferation (Gulati and Thomas, 2007). The majority of these different stimuli (except amino acids) signals to mTORC1 through the modulation of Tuberous sclerosis complex 1 and 2 (TSC1 and TSC2) activity (Gulati et al., 2008). mTORC1 is also the only complex sensitive to acute rapamycin treatment and has been shown to control protein synthesis via the S6 kinase/S6 axis and 4E-BP1 phosphorylation (Sonenberg and Hinnebusch, 2009).

At a physiological level, the mTORC1 signaling pathway has been described to play an important role in the control of energy metabolism, particularly in lipid biosynthesis (Inoki et al., 2012). This notion has emerged from observations of clinical trials involving rapamycin or rapalog administration. Side effects of these drugs have been reported such as hyperlipidemia and hypercholesterolemia and activation of gluconeogenesis in liver, a major organ for lipid biosynthesis (Houde et al., 2010; Levy et al., 2006; Morrisett et al., 2002). Furthermore, rodents treated with rapamycin and rapalogs develop nonalcoholic fatty livers (NAFLs) associated with elevated free fatty acid (FFA) levels (Patsenker et al., 2011). The mechanism by which inhibitors of mTOR generate an increase in lipogenesis involves a multitude of factors that includes PPARγ, SREBP1, and/or lipin1 that interplay with each other to regulate the lipogenic gene program (Peterson et al., 2011).

Aside from the well-established role of mTOR as a kinase in signaling cascades, several studies have shown that mTOR can shuttle between the cytoplasm and nucleus (Bachmann et al., 2006; Kim and Chen, 2000; Rosner and Hengstschläger, 2008; Zhang et al., 2002). Standard chromatin immunoprecipitation (ChIP) studies revealed that mTOR is recruited to DNA and can interact with various transcription factors such as YY1 and MAF1 to modulate gene expression at a transcriptional level (Cunningham et al., 2007; Kantidakis et al., 2010). Although both mTORC1 and mTORC2 components have been identified in the nucleus (Rosner and Hengstschläger, 2008), mTOR recruitment to DNA has been shown to be sensitive to amino acid levels and rapamycin treatment (Tsang et al., 2010), indicating that mTOR occupancy on chromatin is mTORC1-dependent. In addition, TOR1 has been shown to bind DNA in yeast (Li et al., 2006), and Raptor occupancy on chromatin has been observed previously (Cunningham et al., 2007; Shor et al., 2010). Although the first de novo mTOR target genes identified

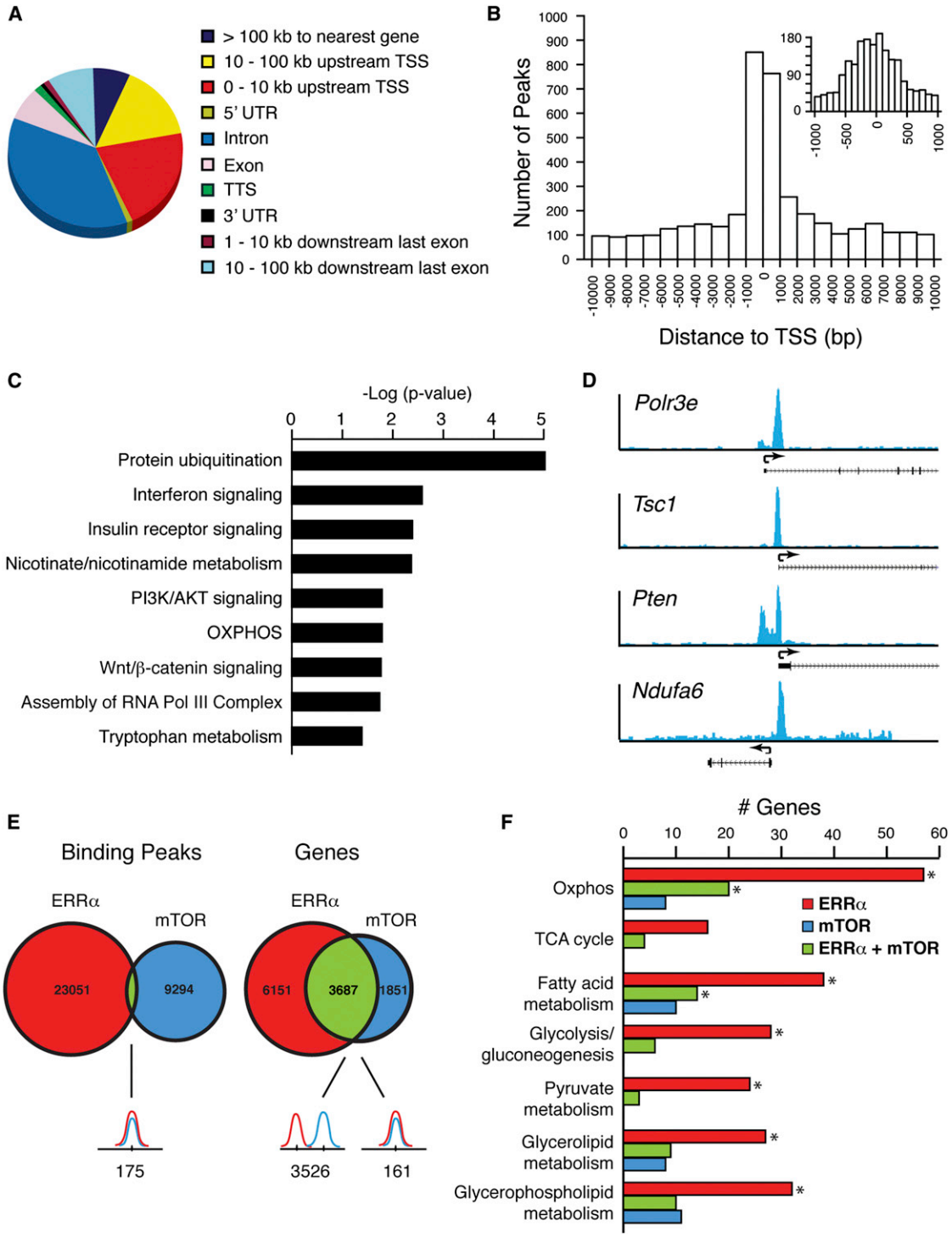

Figure 1. mTOR Is a Transcriptional Regulator of Metabolic Pathways

(A) Mapping of mouse liver mTOR ChIP-seq peaks across the genome. TTS (transcription termination site) represents binding peaks found −100 bp to + 1 kb relative to the nearest TSS.

(B) Histogram illustrating the distribution of mTOR ChIP-seq peaks ± 10 kb relative to the TSS of the nearest gene. Peaks were combined into 1,000 bp bins. Inner histogram shows peaks ± 1 kb relative to the TSS of the nearest gene. Peaks were combined into 100 bp bins.

(C) Subset of significantly enriched canonical pathways identified by IPA analysis of mTOR ChIP-seq targets found within ± 10 kb relative to the TSS of the nearest gene.

(D) Graphical view of mTOR ChIP-seq binding peaks (tag densities) around the TSSs of the genes *Polr3e*, *Tsc1*, *Pten*, and *Ndufa6* obtained from the UCSC genome browser. Arrows show direction of transcription.

(legend continued on next page)

were polymerase III (pol III)-dependent genes, mTOR was later shown to bind to the gene encoding dystrophin, and two genes encoding proteins involved in mitochondrial function, cytochrome C and the coactivator PGC-1α (Cunningham et al., 2007; Kantidakis et al., 2010; Risson et al., 2009; Shor et al., 2010; Tsang et al., 2010). While these findings suggested a distinct mechanism by which mTOR could regulate energy metabolism, the limited number of mTOR target genes identified thus far currently prevents a full appreciation of the importance of the potential role of mTOR as a transcriptional regulator.

Estrogen-related receptor α (ERRα, NR3B1) is an orphan nuclear receptor that plays a crucial role in the transcriptional control of mitochondrial function and energy metabolism (Deblois and Giguère, 2011; Eichner and Giguère, 2011; Giguère, 2008; Villena and Kralli, 2008). The identification of the first ERRα target gene, *Acadm*, encoding medium-chain acyl coenzyme A, suggested a potential role for ERRα in the control of lipid metabolism (Sladek et al., 1997; Vega and Kelly, 1997). Mice lacking ERRα are lean and resistant to weight gain under a high-fat diet (Luo et al., 2003). Furthermore, ERRα is a regulator of glucose homeostasis. ERRα-null mice exhibit time-dependent hypoglycemia and hypoinsulinemia with enhanced glucose uptake due to increased insulin sensitivity (Dufour et al., 2011). In agreement with the findings obtained in ERRα-null mice, administration of a highly selective ERRα inverse agonist (compound 29, C29) in rodent models of obesity and diabetes results in improved insulin sensitivity and glucose tolerance accompanied by reduced circulating glucose, FFA, and triglyceride (TG) levels (Patch et al., 2011). These observations have reinforced the concept that ERRα is an essential factor in the control of energy metabolism and thus a potential therapeutic target for the treatment of metabolic disorders (Giguère, 2008).

While mTOR and ERRα are considered as key regulators of metabolism, particularly in mitochondrial function and lipid homeostasis, it is currently unknown to which extent the two signaling pathways intersect. Herein, we demonstrate that mTOR targets metabolic genes on a genome-wide scale and positively regulates ERRα expression and activity via transcriptional control of the ubiquitin pathway. We further show that the mTOR/ERRα axis is of physiological significance as it plays a key role in the development of rapamycin-induced NAFL.

RESULTS

A Transcriptional Network Linking mTOR and ERRα to the TCA Cycle and Lipid Metabolism

To explore whether mTOR plays a global role as a transcriptional regulator and its potential interplay with the ERRα regulatory pathway, we performed mTOR and ERRα ChIP-sequencing (ChIP-seq) analyses using chromatin obtained from mouse livers (Table S1, Table S2, Table S3, and Table S4 available online). Analysis of the data sets revealed 9,469 peaks bound by mTOR. The distribution of these binding events across the genome is shown in Figure 1A. We first investigated the extent of mTOR recruitment to pol-III-driven genes by comparing our mTOR ChIP-seq data set with a recently published pol III ChIP-seq data set (Carrière et al., 2012). Comparison of the two data sets revealed that 44% of the pol-III-bound RNA-encoding genes are also bound by mTOR (Figure S1A). Our analysis demonstrates a striking preference for shared pol III/mTOR occupancy of 4.5S RNAs (100%) and transfer RNAs (tRNAs; 76%) compared to SINEs (3%) (Table S5). Standard ChIP analysis validates that mTOR is recruited to different classes of RNA-encoding genes bound by pol III (Figures S1B and S1C). We next examined the mTOR ChIP-seq data set for mTOR binding to pol-II-transcribed genes. Validation by standard ChIP analysis of a subset of these genes is shown in Figure S1D. A total of 4,055 of the 9,469 mTOR-bound peaks associated with 54% (2,969) of the unique genes identified are found within ± 10 kb of the transcriptional start sites (TSSs) of genes (Figure 1B). These binding events have a preference for a region surrounding ± 1kb of TSSs of genes (Figures 1B and S1E). Analysis of mTOR target genes revealed an enrichment in physiological functions related to protein metabolism and turnover including the protein ubiquitination pathway, assembly of RNA pol III complex and tryptophan metabolism (Figure 1C). We also found a significant enrichment of genes involved in the PI3K/AKT, Wnt/β-catenin, and insulin receptor signaling pathways, findings that are consistent with the known roles of mTORC1. In addition, mTOR is significantly recruited at genes involved in oxidative phosphorylation (OXPHOS) (Figure 1C). Prototypic binding profiles illustrating mTOR recruitment to genes involved in these various processes are shown in Figure 1D. Next, we investigated whether mTOR occupancy of pol-III- and pol-II-transcribed genes is dependent on the presence of the mTORC1-specfic protein, Raptor. mTOR ChIP assays performed on livers from Raptor$^{+/-}$ mice revealed less recruitment of mTOR to target genes when Raptor levels are diminished in vivo (Figures S2A and S2B). Known and de novo motif finding analyses did not identify with high confidence a consensus motif specifically associated with mTOR binding events.

Mouse liver ERRα ChIP-seq analyses identified 23,226 peaks significantly enriched for the sequence 3′-TCAAGGTCA-5′, the known ERRα consensus binding motif (Sladek et al., 1997) (Figure S3A). Nearly 50% of the peaks were found within intronic regions with a substantial preference for the first intron close to the TSS (Figures S3A and S3B). A total of 8,077 ERRα-bound peaks are found within ± 10 kb of the TSSs of genes corresponding to 43% (2,373) of the unique genes identified (Figure S3C). Investigation of a potential crosstalk between ERRα and mTOR by comparing the two ChIP-seq data sets did not show a significant overlap in binding peaks implying that ERRα and mTOR do not interact with each other on DNA (Figure 1E). In contrast, a significantly large proportion of mTOR target genes (3,687) are also targeted by ERRα, indicating that the two factors regulate common biological functions. As shown in Figure 1F, ERRα and mTOR are commonly recruited to genes involved in

(E) Venn diagrams illustrating the overlap in number of binding peaks and unique genes identified in the ERRα and mTOR mouse liver ChIP-seq data sets.
(F) Number of ChIP-seq targets bound by either ERRα (red), mTOR (blue) or both (green) within metabolic pathways identified by IPA analysis are shown.
*$p < 0.05$.
See also Figures S1–S3 and Table S1, Table S2, Table S3, Table S4, and Table S5.

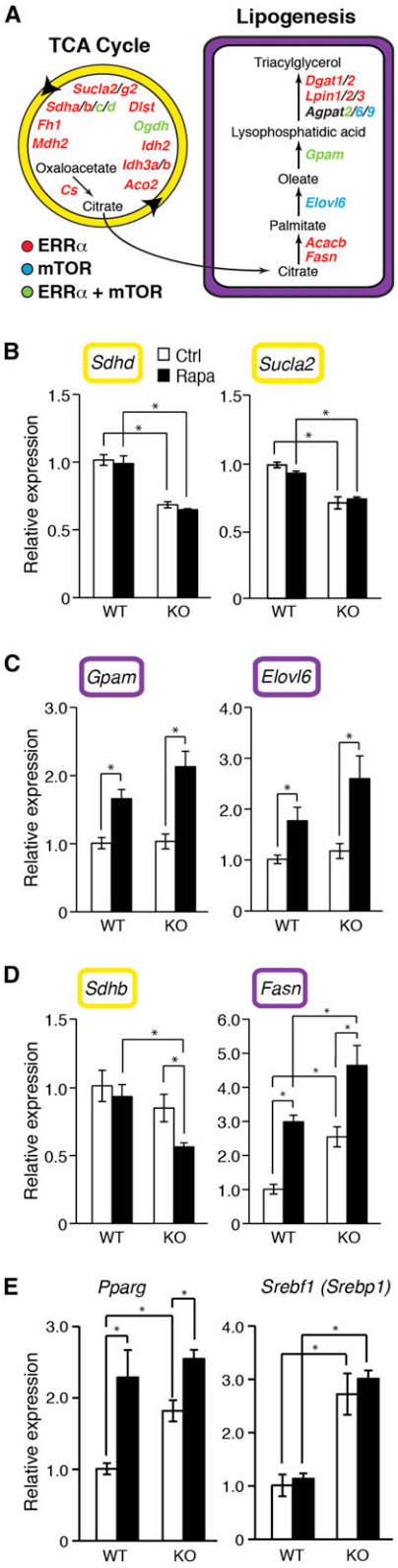

Figure 2. Crosstalk between mTOR and ERRα in the Transcriptional Control of the TCA Cycle and Lipogenesis

(A) Schematic illustrating the ChIP-seq targets bound by ERRα (red), mTOR (blue), or both (green) implicated in the TCA cycle and lipid biosynthesis.

metabolic processes, including OXPHOS, the TCA cycle, glycolysis/gluconeogenesis, and lipid metabolism.

We next sought to determine the impact of mTOR and ERRα signaling on the hepatic expression of a subset of mTOR and/or ERRα targeted genes involved in the TCA cycle and lipogenesis (Figure 2A). Our results uncovered three different classes of genes based on their response to rapamycin inhibition of mTOR and/or ablation of ERRα. First, we identified genes that are only affected by the loss of ERRα that includes *Sdhd* and *Sucla2* whose gene products are enzymes of the TCA cycle (Figure 2B). Second, *Gpam* and *Elovl6,* whose gene products are implicated in the lipogenic pathway, were classified as being only sensitive to rapamycin (Figure 2C). Rapamycin treatment resulted in increased mRNA levels of these two genes irrespective of the genotype of the mice. Finally, *Sdhb* and *Fasn*, whose gene products are involved in the TCA cycle and in the lipid biosynthesis pathway, respectively, were classified based on their responsiveness to a combined loss of ERRα and mTOR activity. *Sdhb* responded only to a combined loss in both ERRα and mTOR activity while *Fasn* responded in an additive manner to both ERRα and mTOR modulation (Figure 2D). In particular, livers of ERRα-null mice were found to have nearly 2.5 times more *Fasn* levels compared to wild-type (WT) and these mRNA levels nearly doubled again in the presence of rapamycin. As *Fasn* is a direct target of ERRα but not mTOR, the further increase in *Fasn* transcript levels in ERRα-knockout (KO) mice by rapamycin indicates that other transcription factors could also play a role in the control of this gene. Indeed, the effects of rapamycin treatment and/or loss of ERRα on *Pparg* expression is similar to that observed for *Fasn* (Figure 2E). While rapamycin treatment did not affect *Srebf1* (encoding Srebp1) expression, levels were nearly tripled in ERRα-null mice. In addition, an induction of *Ppara* levels was observed in the ERRα-null livers, which could be a response to the compensatory increase of *Ppargc1a* expression (Figure S4).

Loss of ERRα Activity Results in Impaired TCA Cycle Activity and Exacerbates Rapamycin-Induced NAFL

We next explored the biological consequence of both rapamycin-mediated inhibition of mTOR activity and loss of ERRα in mouse liver. First, we examined that impact on TCA cycle activity by quantifying hepatic TCA cycle intermediates (Figure 3). In addition, the expression level of one gene for every step of the TCA cycle was measured. Of note, most of these genes belong to the subgroup of genes responding to both rapamycin and the absence of ERRα (Figure 2D). Treatment of WT mice with rapamycin did not significantly affect the levels of the TCA intermediates measured. In contrast, ERRα-null mice exhibit higher levels

(B) Quantitative RT-PCR (qRT-PCR) analysis of metabolic genes that are ERRα-responsive in livers isolated from WT and ERRα-null mice treated with or without rapamycin for 7 days. Data are normalized to *Hprt* levels. Error bars represent ± SEM. *p < 0.05.

(C) qRT-PCR analysis of metabolic genes that are rapamycin-responsive. Error bars represent ± SEM. *p < 0.05.

(D) qRT-PCR analysis of metabolic genes that are responsive to a combined loss of ERRα and rapamycin. Error bars represent ± SEM. *p < 0.05.

(E) qRT-PCR analysis of metabolic transcription factors that are responsive to ERRα and/or rapamycin. Error bars represent ± SEM. *p < 0.05.

See also Figure S4 and Table S8.

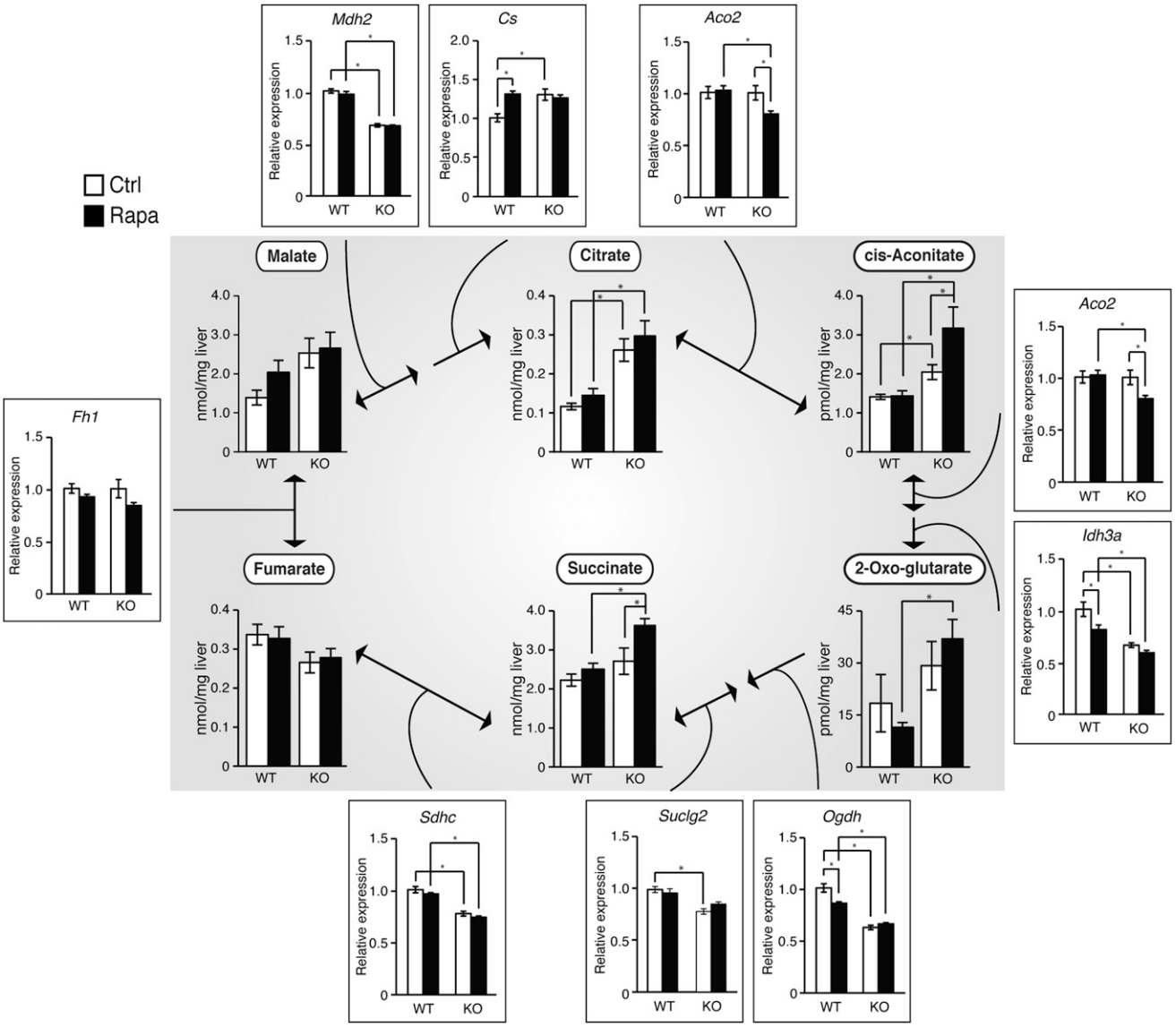

Figure 3. Metabolic Crosstalk between mTOR and ERRα in the Production of TCA Cycle Intermediates

Quantification of TCA cycle intermediates by either GC/MS or NMR analyses of livers collected from wild-type and ERRα-KO mice administered rapamycin (10 mg/kg) or vehicle on a daily basis by intraperitoneal injection during a 7 day period (inside gray area). qRT-PCR analysis was performed on the same livers used for metabolomics studies, and one TCA cycle gene at every step in the cycle is shown as boxed graphs. qRT-PCR data are normalized to *Hprt* levels. Error bars represent ± SEM. *$p < 0.05$. See also Table S8.

of citrate and *cis*-aconitate. Furthermore, rapamycin treatment in ERRα-null mice resulted in increased levels of *cis*-aconitate and succinate with a trend for higher 2-oxo-glutarate levels compared to untreated ERRα-KO mice. Interestingly, intermediates did not accumulate in later stages of the TCA cycle, and no further accumulation of citrate was observed. The repressed gene expression profiles in the ERRα-KO livers of the enzymes corresponding to the transitions from citrate through to fumarate suggests that the specific metabolite accumulation observed indicates the outcome of an ERRα-dependent blunted TCA cycle between these steps.

Metabolomic data suggests that rapamycin treatment in ERRα-KO mice might result in increased incorporation of citrate into the lipogenic pathway. To test this hypothesis, we performed histological and biochemical analyses on the corresponding livers. As expected, rapamycin treatment reduced the phosphorylation of the ribosomal S6 protein in both genotypes (Figure 4A). In addition, we found that the phosphorylation of AKT, a target of mTORC2, was higher in all of the rapamycin-treated mice, a phenomenon previously noted in the liver (Sarbassov et al., 2006). There were no noticeable differences in basal S6 or AKT phosphorylation between the WT and KO mice, suggesting that the loss of ERRα does not affect the mTOR signaling pathway. Surprisingly, rapamycin treatment in WT mice nearly completely abolished ERRα protein levels (Figure 4A) in a manner that cannot be explained by the modest

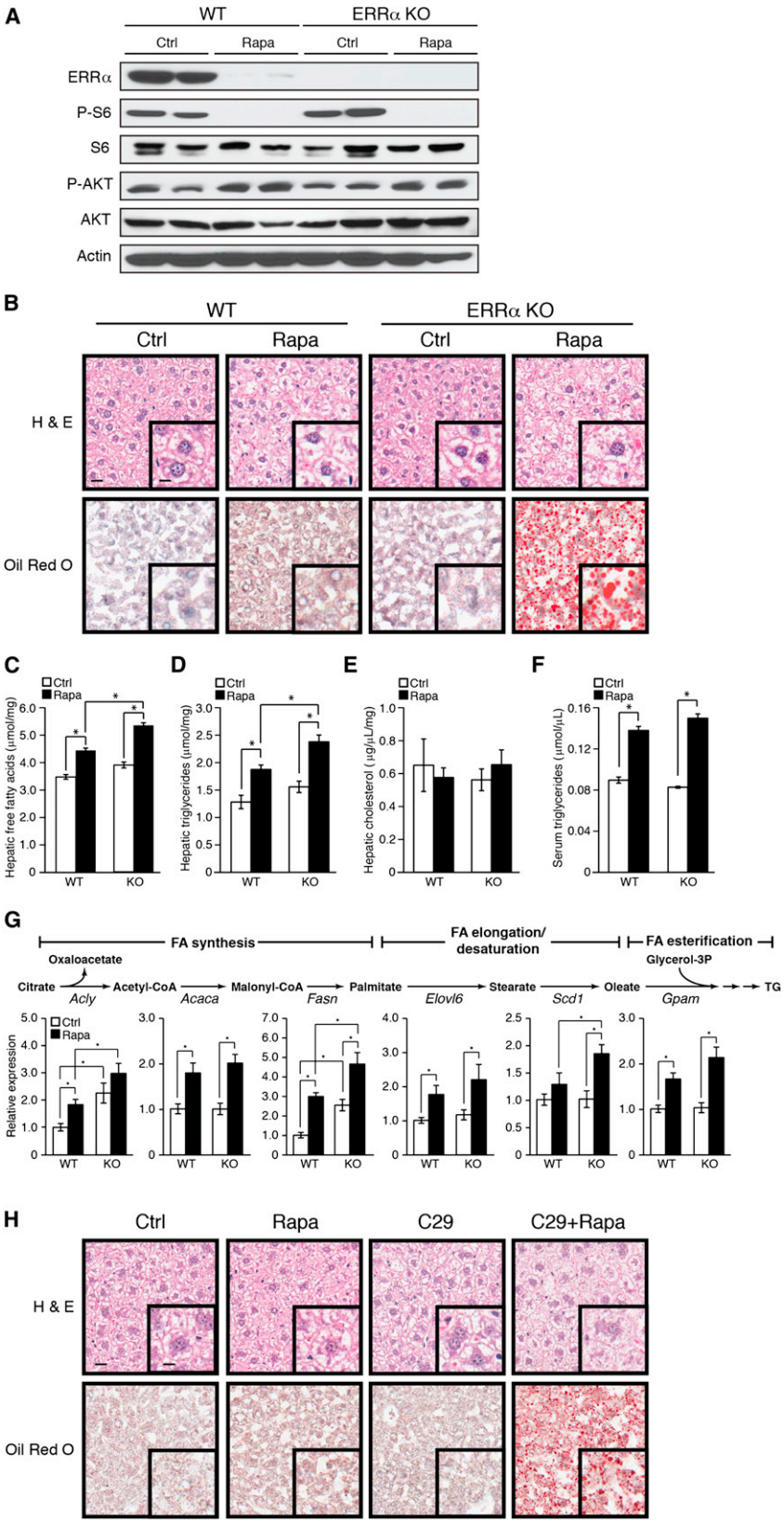

Figure 4. Rapamycin-Induced NAFL Is Exacerbated by Genetic and Pharmacological Inhibition of ERRα

(A) Western blot analysis of total ERRα, phospho-S6 (S235/S236), total S6, phospho-AKT (S473), and total AKT levels in mouse livers collected from wild-type and ERRα-KO mice treated with or without rapamycin for 7 days. Actin levels are shown as a loading control.

(B) Representative hematoxylin and eosin (H&E) and oil red O staining of liver sections from wild-type and ERRα-KO mice administered rapamycin (10 mg/kg) or vehicle on a daily basis by intraperitoneal injection during a 7 day period. Scale bars represent 40 μm and 160 μm (inset).

(C) Measurement of hepatic FFAs of WT and ERRα-null mice after a 7 day treatment of rapamycin or vehicle. Error bars represent ± SEM. *$p < 0.05$.

(D) Measurement of hepatic TGs of WT and ERRα-null mice as in (C).

(E) Measurement of hepatic cholesterol levels of WT and ERRα-null mice as in (C).

(F) Measurement of serum TG levels in WT and ERRα-null mice as in (C).

(G) qRT-PCR analysis of genes at each of the first six steps in the conversion of citrate to TGs on livers isolated from WT and ERRα-null mice treated with or without rapamycin for 7 days. Data are normalized to *Hprt* levels. Error bars represent ± SEM. *$p < 0.05$.

(H) Representative H&E and oil red O staining of liver sections from WT mice administered rapamycin (10 mg/kg), the ERRα inverse agonist C29 (10 mg/kg), or both on a daily basis by intraperitoneal injection during a 10 day period. Scale bars represent 40 μm and 160 μm (inset).

See also Figures S4 and S5 and Table S8.

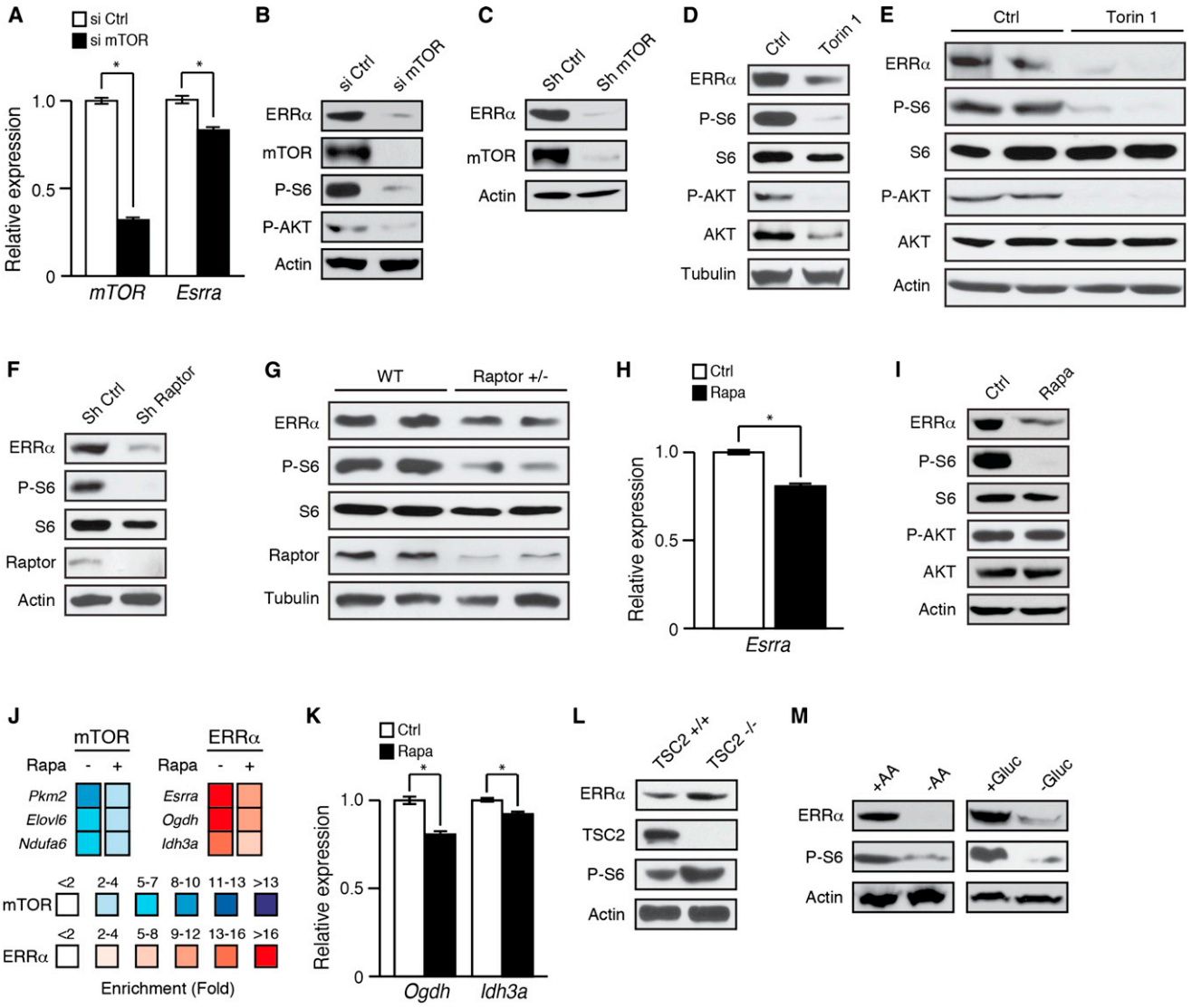

Figure 5. ERRα Expression and Activity Is Regulated by the mTOR Signaling Pathway

(A) qRT-PCR expression analysis of *mTOR* and *Esrra* expression after treatment of Hepa 1-6 cells with a pool of siRNAs against mTOR for 96 hr. Data are normalized to *Hprt* levels. Error bars represent ± SEM. *p < 0.05.

(B) Western blot analysis of total ERRα, mTOR, phospho-S6 (S235/S236), and phospho-AKT (S473) in Hepa 1-6 cells treated with a pool of siRNAs for 96 hr against mTOR. Actin levels are shown as a loading control.

(C) Western blot analysis shows loss of ERRα protein levels in HeLa cells infected with an shRNA targeting mTOR for 72 hr. Actin levels are shown as a loading control.

(D) Total ERRα, phospho-S6 (S235/S236), total S6, phospho-AKT (S473), and total AKT protein levels in Hepa 1-6 cells in response to a 24 hr treatment of torin 1. Tubulin levels are shown as a loading control.

(E) Western blot analysis of total ERRα, phospho-S6 (S235/S236), total S6, phospho-AKT (S473), and total AKT levels in mouse livers collected from WT mice treated with vehicle or torin 1 on a daily basis by intraperitoneal injection during a 2 day period. Actin levels are shown as a loading control.

(F) Western blot analysis of total ERRα, phospho-S6 (S235/S236), total S6, and Raptor levels in Hepa 1-6 cells infected with control shRNA or shRNA directed against Raptor for 7 days. Actin levels are shown as a loading control.

(G) Western blot analysis of total ERRα, phospho-S6 (S235/S236), total S6, and Raptor protein levels in wild-type and Raptor$^{+/-}$ mouse livers. Tubulin levels are shown as a loading control.

(H) *Esrra* mRNA expression levels in Hepa 1-6 cells cells treated with rapamycin or vehicle for 48 hr. Data are normalized to *Hprt* levels. Error bars represent ± SEM. *p < 0.05.

(I) Total ERRα, phospho-S6 (S235/S236), total S6, phospho-AKT (S473), and total AKT protein levels in Hepa 1-6 cells in response to a 48 hr treatment of rapamycin. Actin levels are shown as a loading control.

(J) Standard ChIP analyses of mTOR and ERRα binding to their respective metabolic target genes in Hepa 1-6 cells treated with rapamycin or vehicle as a control for 48 hr.

(K) qRT-PCR analysis of *Ogdh* and *Idh3a* expression in Hepa 1-6 cells treated with rapamycin or vehicle for 48 hr. Data are normalized to *Hprt* levels. Error bars represent ± SEM. *p < 0.05.

(legend continued on next page)

decrease in *Esrra* transcript levels alone (Figure S4). These observations suggest that rapamycin affects ERRα expression predominantly at the posttranslational level. Histological examination showed a greater microvesicular accumulation of lipids in ERRα-KO livers compared to WT in response to rapamycin (Figure 4B). Although no significant difference in basal liver FFAs and TGs were identified in ERRα-null livers, ERRα-KO mice treated with rapamycin exhibited an increase in hepatic FFA and TG content compared to rapamycin treated WT mice (Figures 4C and 4D). In contrast, no differences in liver cholesterol levels were observed between the four groups (Figure 4E). Moreover, rapamycin-treated mice had significantly more circulating serum TG levels independent of the genotype (Figure 4F). Next, we analyzed the mRNA levels of the genes controlling the first six steps involved in the conversion of citrate to TGs (Figure 4G). Overall, levels of *Acly* as well as *Fasn* and *Scd1* were found to be highest in ERRα-null mice treated with rapamycin. Of interest, loss of *Scd1* expression in mice is associated with decreased lipogenesis and increased fatty acid oxidation (FAO), leading to a protective effect against the development of hepatic steatosis (Cohen et al., 2002). Furthermore, *Acaca* (encoding ACC1) mRNA levels were significantly increased in both WT and ERRα-null mice in a rapamycin-dependent manner reflecting the development of NAFLs in these mice (Figure 4G). No differences in *Acacb* (encoding ACC2) levels were found. However, rapamycin induced both phosphorylation of AMPKα and its target ACC (Figure S5A). Despite an apparent attempt to inhibit lipogenesis and stimulate FAO, these mice nonetheless develop NAFLs. For further validation of our findings that rapamycin treatment in mice deficient in ERRα activity worsens the development of NAFLs, mice were injected with rapamycin and/or the ERRα inverse agonist C29 (Patch et al., 2011). As observed in mice with a genetic ablation of ERRα, larger vesicles and higher accumulation of lipids were found in livers of cotreated mice (Figure 4H). Moreover, we investigated whether the potent mTOR inhibitor, torin 1, capable of suppressing both mTORC1 and mTORC2 complexes can also exacerbate the development of NAFLs in mice lacking ERRα. Because of the unexpected lethal toxicity of torin 1 administration specifically observed in ERRα-null mice likely due to lipotoxicity, livers were collected after a 2-day administration of torin 1. Histological analysis of liver sections revealed severe lipid accumulation in torin 1-treated ERRα-null mice (Figure S5B). Taken together, these data exclude the possibility that the increased lipid accumulation in the livers of rapamycin- and torin-1- treated ERRα-null mice is due to a life-long absence of ERRα.

mTOR Signaling Controls ERRα Expression and Transcriptional Activity

The observation that the expression of ERRα is regulated in a rapamycin-sensitive manner led us to investigate the molecular link between mTORC1 signaling and ERRα transcriptional activity. At the mRNA level, treatment of the Hepa 1-6 mouse cell line with small interfering RNAs (siRNAs) against mTOR resulted in a modest but significant reduction (~20%) in ERRα transcript levels (Figure 5A). Consistent with what we observed previously in livers of rapamycin-treated mice, ERRα protein expression was strongly abrogated in cells lacking mTOR (Figure 5B). Similar results were obtained in a human cell line (HeLa) infected with short hairpin RNA (shRNA) directed against human mTOR (Figure 5C). Moreover, inhibition of both mTORC1 and mTORC2 activity by torin 1 treatment in Hepa 1-6 cells and in mice also results in a significant reduction in ERRα protein levels (Figures 5D and 5E). Targeted disruption of mTORC1 signaling in Hepa 1-6 cells infected with mouse specific shRNA against Raptor also resulted in loss of ERRα protein levels (Figure 5F). Similarly, a reduction in ERRα protein expression was observed in livers of Raptor$^{+/-}$ mice compared to WT (Figure 5G). Treatment of Hepa 1-6 cells with the mTORC1 inhibitor, rapamycin, results in a similar decrease in ERRα mRNA levels to that observed previously with siRNAs against mTOR (Figure 5H). Interestingly, rapamycin treatment also resulted in a strong decrease in ERRα protein levels in these cells (Figure 5I). Next, we sought to determine whether the effects of rapamycin on ERRα also altered recruitment of ERRα to its target genes. First, we determined whether rapamycin treatment in Hepa 1-6 cells alters mTOR recruitment to DNA. Indeed, we observed a reduction in mTOR binding to metabolic target genes in response to rapamycin treatment (Figure 5J). In parallel, we found decreased ERRα recruitment to its own promoter, *Esrra*, as well as to that of two metabolic targets, *Ogdh* and *Idh3a*, in rapamycin-treated cells (Figure 5J), coinciding with the reduction in the mRNA levels of these genes in Hepa 1-6 cells (Figures 5H and 5K) or mouse liver (Figure 3) exposed to rapamycin. To further validate the influence of mTORC1 on ERRα expression, we tested the effects of manipulating mTORC1 activity by either a genetic approach or physiological stimuli. Constitutive activation of mTORC1 signaling in TSC2-null mouse embryonic fibroblasts (MEFs) results in an increase in ERRα levels (Figure 5L), while inhibition of mTORC1 activity via starvation of Hepa 1-6 cells of either amino acids or glucose abolished ERRα expression in those cells (Figure 5M).

Rapamycin Induces Ubiquitin/Proteasome-Mediated ERRα Degradation

We next explored the underlying mechanism responsible for the striking decrease in ERRα protein expression in response to inhibition of mTOR signaling. To test whether mTOR inhibition contributes to ERRα degradation via a ubiquitin-dependent mechanism, we first examined the effect of mTOR silencing on whole-cell protein ubiquitination (Figure 6A). mTOR knockdown resulted in decreased phospho-S6, mTOR, and ERRα protein levels associated with a higher amount of ubiquitinated proteins compared to the cells transfected with siCtrl. In the presence of rapamycin, nuclear ERRα was depleted after drug treatment (Figure 6B). Of note, rapamycin treatment resulted in decreased

(L) Activation of mTOR signaling in TSC2-null MEFs results in increased ERRα and phospho-S6 (S235/S236) protein levels as determined by western blot analysis. Actin levels are shown as a loading control.
(M) Western blot analysis shows loss of ERRα and phospho-S6 (S235/S236) protein levels in Hepa 1-6 cells after a 24 hr starvation of total amino acids or glucose. Actin levels are shown as a loading control.
See also Tables S6–S8.

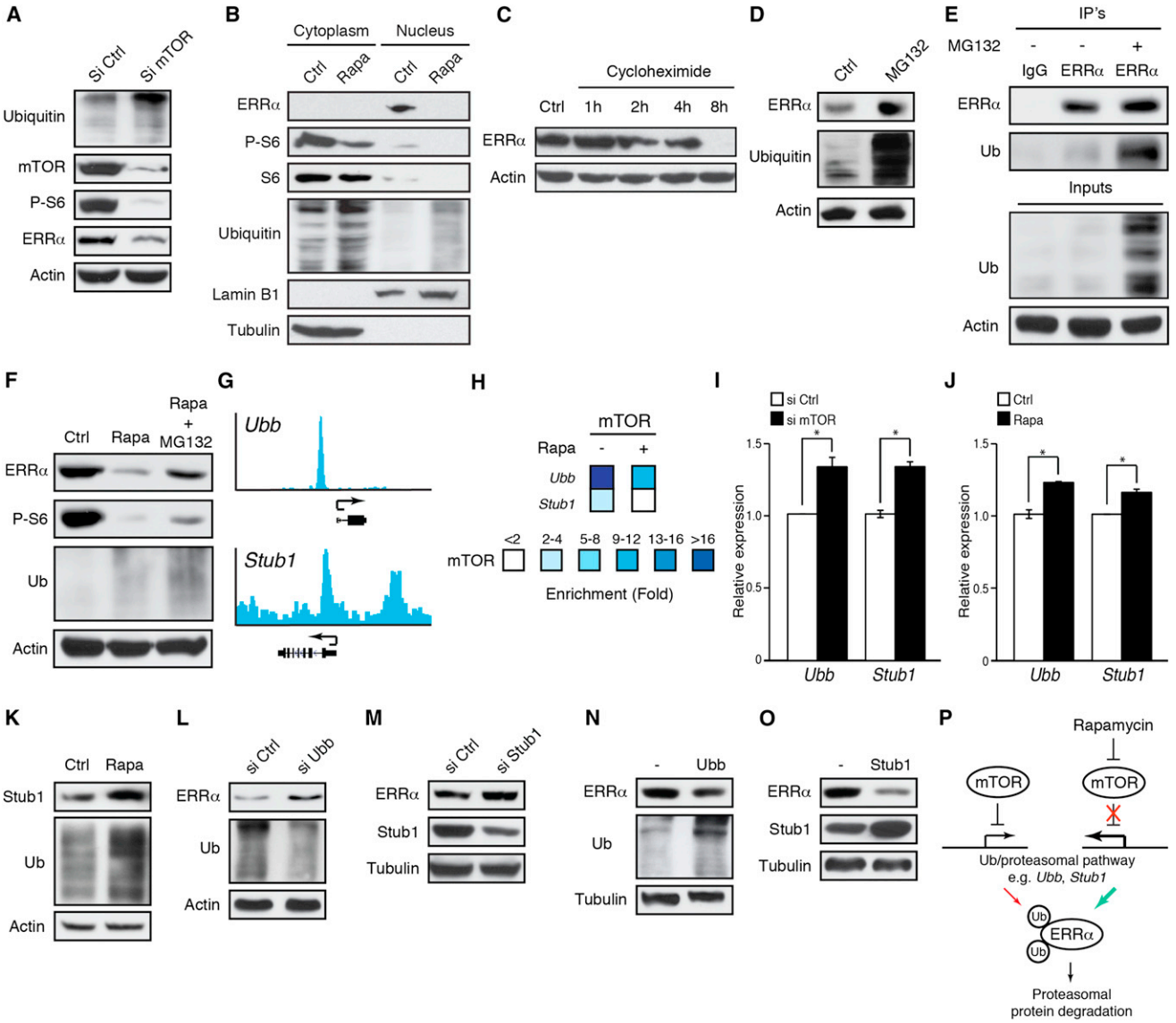

Figure 6. mTOR-Mediated Degradation of ERRα via a Ubiquitin/Proteasomal-Dependent Mechanism

(A) Western blot analysis of total ubiquitinated proteins, mTOR, phospho-S6 (S235/S236), and ERRα in Hepa 1-6 cells treated with a pool of siRNAs against mTOR. Actin levels are shown as a loading control.

(B) Western blot analysis of ERRα, phospho-S6 (S235/S236), total S6, and ubiquitinated proteins in nuclear and cytoplasmic fractions of Hepa 1-6 cells treated with rapamycin or vehicle for 48 hr. Lamin B1 and tubulin levels are shown as loading controls for nuclear and cytoplasmic fractions, respectively.

(C) Western blot analysis of ERRα expression in Hepa 1-6 cells treated with cycloheximide at the indicated time points. Actin levels are shown as a loading control.

(D) Hepa 1-6 cells were treated with or without the proteasome inhibitor, MG132 for 24 hr. Western blot analysis shows an accumulation of ubiquitinated proteins and ERRα in the presence of MG132. Actin levels are shown as a loading control.

(E) Immunoprecipitation studies show ERRα ubiquitination in Hepa 1-6 cells treated with MG132 for 24 hr. Actin levels are shown as a loading control.

(F) Western blot analysis shows that MG132 treatment rescues rapamycin-mediated inhibition of ERRα and phospho-S6 (S235/S236) levels in Hepa 1-6 cells.

(G) Graphical view of mTOR ChIP-seq binding peaks (tag densities) around the TSSs of *Ubb* and *Stub1* (*CHIP*) obtained from the UCSC genome browser. Arrow shows direction of transcription.

(H) Standard ChIP analysis of mTOR recruitment to *Ubb* and *Stub1* (*CHIP*) target genes in Hepa 1-6 cells treated with rapamycin or vehicle as a control for 48 hr.

(I) qRT-PCR analysis of *Ubb* and *Stub1* (*CHIP*) mRNA levels in Hepa 1-6 cells treated with siRNAs against mTOR for 96 hr. Data are normalized to *Hprt* levels. Error bars represent ± SEM. *$p < 0.05$.

(J) Loss of mTOR signaling in Hepa 1-6 cells via rapamycin treatment leads to an increase in both *Ubb* and *Stub1* (*CHIP*) mRNA levels. Data are normalized to *Hprt* levels. Error bars represent ± SEM. *$p < 0.05$.

(K) Western blot analysis shows increased Stub1 protein levels in Hepa 1-6 cells treated with rapamycin for 48 hr. Actin levels are shown as a loading control.

(L) Total ERRα and ubiquitinated protein levels in Hepa 1-6 cells treated with a pool of siRNAs against Ubb for 72 hr. Actin levels are shown as a loading control.

(M) Total ERRα and Stub1 (CHIP) protein levels in Hepa 1-6 cells treated with a pool of siRNAs against Stub1 for 72 hr. Tubulin levels are shown as a loading control.

(legend continued on next page)

P-S6 in both cytoplasmic and nuclear fractions. In parallel, we noticed an accumulation of ubiquitinated proteins in both cellular fractions in response to the mTOR inhibitor. These data indicate that mTOR inhibition leads to an activation of the ubiquitin pathway in hepatocytes. We next determined the turnover of ERRα in hepatocytes. Cycloheximide treatment shows that the ERRα protein has a relatively short half-life (~4 hr) (Figure 6C). Inhibition of the proteasome with MG132 led to an increase in both ERRα and its ubiquitinated form (Figures 6D and 6E). Interestingly, MG132 treatment was also found to protect against rapamycin-induced ERRα protein degradation and rescued some of the rapamycin inhibition of S6 phosphorylation (Figure 6F).

Next, we investigated whether mTOR regulates the protein ubiquitination pathway directly, the most significantly enriched canonical pathway identified among the mTOR ChIP-seq target genes (Figure 1C). Binding peak profiles of mTOR for the genes *Ubb* and *Stub1*, also known as CHIP, encoding ubiquitin B and an E3-ubiquitin protein ligase, respectively, are shown in Figure 6G. To determine whether mTOR regulates the expression of *Ubb* and *Stub1*, we first show that mTOR recruitment to the *Ubb* and *Stub1* genes is rapamycin sensitive (Figure 6H). Second, Hepa 1-6 cells treated with siRNAs directed against mTOR led to an upregulation in both *Ubb* and *Stub1* expression (Figure 6I). Similarly, rapamycin treatment in Hepa 1-6 cells resulted in increased mRNA levels of both *Ubb* and *Stub1* with a parallel increase in Stub1 and total ubiquitin protein levels (Figures 6J and 6K). Moreover, siRNA-mediated knockdown or overexpression of either *Ubb* or *Stub1* in Hepa 1-6 cells resulted in an increase or decrease in ERRα protein levels, respectively (Figures 6L–6O). Our results demonstrate that mTOR signaling controls ERRα degradation by regulating the nonlysosomal ubiquitin/proteasome system at the transcriptional level (Figure 6P).

DISCUSSION

ERRα is well known to play a pivotal role in the control of energy metabolism and, like mTOR, is a potential therapeutic target for the treatment of metabolic disorders. The work presented herein reveals that mTOR and ERRα bind to and control the expression of a large set of both unique and common genes implicated in mitochondrial function and the lipid biosynthesis pathway. Furthermore, we show that rapamycin inhibition of mTOR leads to the degradation of ERRα through a proteasome-dependent mechanism, indicating that ERRα is integrated into the mTOR signaling pathway. The finding that rapamycin represses ERRα expression identifies an additional molecular link between mTOR and ERRα in the control of energy metabolism. Our data suggest that the metabolic side effects that occur in response to rapamycin treatment are mediated in part through the reduction in ERRα expression. Loss of ERRα activity via genetic or pharmacological inhibition exacerbates the development of rapamycin-induced NAFL.

The absence of ERRα activity results in a significant dysregulation of the expression of genes involved in the TCA cycle and lipogenic pathways in the liver resulting in a seemingly increased potential for hepatic de novo lipogenesis. Despite a tendency for more FAs and TGs, ERRα-null mice were not found to significantly accumulate lipids in the liver. In addition, no increase in circulating TGs was found, suggesting that ERRα-null mice maintain lipid homeostasis by activating compensatory mechanisms to metabolize lipids. While elevated levels of the transcription factors *Pparg* and *Srebp1*, both capable of inducing lipogenic gene programs were observed, loss of ERRα also results in a parallel induction in *Ppargc1a* and *Ppara* levels, two factors known to play a vital role in stimulating FAO. Moreover, ERRα-null mice display a mild increase in both p-AMPKα and p-ACC levels suggesting a decrease in the conversion of acetyl-CoA to malonyl-CoA and a consequent activation of FAO. Although ERRα-null mice accumulate TCA cycle intermediates and thus seem to have decreased mitochondrial function, they do not exhibit dyslipidemia under normal conditions. Further studies are needed to identify the exact mechanisms by which loss of ERRα activity alone does not lead to the development of NAFLs. On the other hand, rapamycin treatment of ERRα-null mice exacerbated the observed NAFL in rapamycin-treated WT mice. Although rapamycin treatment in both WT and ERRα-null mice led to a robust increase in p-AMPKα and p-ACC levels, this compensatory mechanism to inhibit lipogenesis and activate FAO was not sufficient to prevent hyperlipidemia in these mice. Rapamycin-treated ERRα-null mice were found to display higher mRNA levels of *Acly*, *Fasn*, and *Scd1* involved in lipogenesis compared to rapamycin-treated WT mice. Despite the greater accumulation of lipids in ERRα-null mice compared to WT in response to rapamycin, no difference in circulating TG levels was found between the mice, indicating a possible decreased efficiency in mice lacking ERRα to export lipids from the liver. Dysregulation in FA influx into the liver in response to rapamycin might also play a role. In addition, administration of rapamycin to mice lacking ERRα results in a greater accumulation of TCA cycle intermediates compared to ERRα-null mice alone. In contrast, treatment of WT mice with rapamycin had no significant effect on the TCA cycle intermediates measured possibly due to residual ERRα protein and activity. The impaired mitochondrial potential in rapamycin-treated ERRα-null mice suggests a decreased capacity to oxidize lipids despite an observed upregulation in both *Ppargc1a* and *Ppara* levels, and that excess citrate might be reoriented into the lipid biosynthesis pathway. Moreover, as rapamycin induces a diabetic-like state whereby excess energy may be converted into fat, a defect in glucose handling may also be an underlying cause in the observed lipid accumulation in response to rapamycin. Although ERRα is recruited to and can regulate genes of the glycolysis/gluconeogenesis pathway and loss of ERRα correlates with improved insulin sensitivity and glucose tolerance in rodent models (Charest-Marcotte et al., 2010; Dufour et al.,

(N) Total ERRα and ubiquitinated protein levels in Hepa 1-6 cells treated with either empty vector (–) or a vector expressing Ubb for 96 hr. Tubulin levels are shown as a loading control.
(O) Total ERRα and Stub1 (CHIP) protein levels in Hepa 1-6 cells treated with either empty vector (–) or a vector expressing Stub1 for 96 hr as in (B).
(P) Schematic representation highlighting the molecular link between rapamycin, mTOR, ERRα, and the ubiquitin/proteasome system.
See also Figure S6 and Tables S6 and S8.

2011; Patch et al., 2011), absence of ERRα had no effect on rapamycin-induced glucose intolerance in mice. Overall, the data indicate that the exacerbation of rapamycin-induced NAFL in ERRα-null mice compared to WT results from a combination of factors including an increased potential to synthesize lipids, a decreased efficacy in the export of TGs from the liver, and a decreased mitochondrial capacity to metabolize lipids.

The mTOR signaling pathway is one of the major molecular mechanisms controlling protein synthesis and energy metabolism. Recent studies have attributed a nuclear function to mTOR in the transcriptional control of metabolic genes and protein synthesis. However, only a few target genes have been identified to date, and the physiological pathways governed by this transcriptional mechanism remained largely unknown. Our data now show that mTOR specifically targets a large subset of pol-III-transcribed genes (e.g., tRNAs and 4.5S RNAs), supporting its role in protein translation. In addition, mTOR targets a wide-range of pol-II-driven gene programs involved in immune signaling, insulin receptor signaling, cancer signaling pathways, and the ubiquitin/proteasome pathway, as well as OXPHOS and FA metabolism. The mechanisms by which mTOR regulates transcription of these gene networks remains to be elucidated. However, mTOR occupancy of promoter regions was found to be sensitive to both rapamycin and the presence of Raptor, suggesting the involvement of mTORC1 in this molecular process. While it has been previously shown that mTOR can act as a cofactor through phosphorylation of transcription factors such as MAF1 and YY1 (Blättler et al., 2012; Shor et al., 2010), our observation that a clear consensus motif associated with mTOR binding events in the mouse liver genome could not be identified supports the concept that mTOR is a pluripotent cofactor that works with several DNA-binding transcription factors.

Our results demonstrate that ERRα acts downstream of the mTOR signaling pathway and may participate in the mTOR-dependent response toward nutrient availability and energy sensing. We show that rapamycin treatment, which is known to mimic amino-acid-like starvation (Peng et al., 2002), modulates ERRα metabolic target genes (e.g., *Idh3a* and *Ogdh*), supporting a role for ERRα as a component of the mTOR signaling pathway. Although it is clear that loss of ERRα exacerbates rapamycin-induced NAFL, absence of ERRα alone is not sufficient to induce dyslipidemia supporting the requirement for a loss of mTOR activity and the implication of other metabolic regulators in this process. Of note, while the elevated levels of *Esrrg* observed in ERRα-null livers could counteract for the absence of ERRα activity, this compensatory mechanism is lost upon rapamycin treatment (Figure S6A). Indeed, in a manner similar to that observed for ERRα, mTOR inhibition results in the loss of ERRγ in hepatocytes (Figures S6B–S6D). Furthermore, it is well known that mTOR controls energy metabolism through the regulation of SREBP-1. In vitro analyses report an increase in SREBP-1 activity along with the induction of lipogenic genes in an mTORC1- and AKT-dependent manner (Porstmann et al., 2008; Yamauchi et al., 2011). Likewise, studies using adipocyte cell lines demonstrated that mTOR inhibition reduced the mRNA and protein levels of PPARγ. In our work, although rapamycin treatment triggered *Pparg* expression, it did not affect *Srebp1* expression despite a higher level of P-AKT. These results are consistent with published data obtained from adipose tissues of rats treated with rapamycin (Blanchard et al., 2012).

An unanticipated finding of our study is that rapamycin regulates ERRα activity by targeting the receptor for degradation. Our results demonstrate that ERRα is degraded by the nonlysosomal ubiquitin/proteasome system in response to rapamycin and that this effect can be reversed by the proteasome inhibitor MG132. In particular, ChIP-seq and functional analyses revealed that mTOR is recruited to a significant number of genes involved in this process and show that it can repress a subset of these genes, providing a molecular mechanism for the observed rapamycin-induced ERRα degradation in the proteasome. Indeed, rapamycin inhibition of mTOR can promote ubiquitin-conjugation and the degradation of proteins such as Cyclin D1/3 and nitric oxide synthetase (iNOS) (Chotechuang et al., 2011; García-Morales et al., 2006; Harston et al., 2011; Jin et al., 2009). Our work now directly implicates mTOR in this process as a negative transcriptional regulator of the ubiquitination pathway and, together with its known repressive action on autophagy (Kim et al., 2011; Yu et al., 2010), enhances the understanding of its ability to repress protein degradation.

The results presented herein have an important clinical relevance, as analogs of rapamycin (e.g., sirolimus) are commonly used to treat cancer or as immunosuppressants to help prevent the rejection of organ transplants. A significant number of patients treated with these molecules develop associated side effects, including insulin resistance and hepatic hyperlipidemia, also referred to as a diabetes-like syndrome (Levy et al., 2006; Morrisett et al., 2002). Therefore, a better control of glucose homeostasis in these rapamycin-treated individuals has been proposed, in particular by employing antidiabetic drugs as therapeutic strategies to prevent rapalog-induced diabetes (Blättler et al., 2012; Yang et al., 2012). Prior to this study, the use of selective ERRα inverse agonists to improve insulin sensitivity might have been considered to help counteract these side effects (Handschin and Mootha, 2005; Patch et al., 2011). However, genetic and pharmacological evidence presented in this study suggest that treatment of patients with agents inhibiting ERRα, in combination with mTOR inhibitors, would exacerbate the development of NAFLs. Therefore, considering that ERRα-dependent control of metabolic gene programs is rapamycin sensitive, strategies aimed at enhancing rather than repressing ERRα activity appear to be a viable therapeutic avenue to relieve hepatic hyperlipidemia and steatosis observed in patients treated with mTOR inhibitors.

EXPERIMENTAL PROCEDURES

Animals

Two- to 3-month-old male WT, ERRα$^{-/-}$, and Raptor$^{+/-}$ mice in a C57BL/6J genetic background were housed and fed standard chow in an animal facility at McGill University. All mouse manipulations were performed in accordance with the McGill Facility Animal Care Committee and the CCAC. See the Supplemental Experimental Proceduresfor further details.

Metabolomics Analysis

Metabolomics studies were performed at the Metabolomics Core Facility at McGill University. See the Supplemental Experimental Procedures for further details.

Standard ChIP and ChIP Sequencing

mTOR and ERRα standard ChIP enrichments in mouse liver or Hepa 1-6 cells were quantified by qPCR analysis using specific primers and normalized to the average enrichments obtained with two control primer sets amplifying non-mTOR- and -ERRα-bound genomic regions (Tables S6 and S7). For a more detailed description, see the Supplemental Experimental Procedures.

Statistical Analysis

For the comparison between two or three experimental groups, statistical significance was assessed via Student's t test or one-way ANOVA with a Tukey's post test, respectively. Error bars represent ± SEM.

Histology, Biochemistry Measurements, Immunoprecipitation and Western Blotting, Plasmid Transfections, siRNA, Lentiviral shRNA Silencing, and Cell Culture and Reagents

See the Supplemental Experimental Procedures.

ACCESSION NUMBERS

ChIP-seq data have been deposited in the NCBI Gene Expression Omnibus (GEO; http://www.ncbi.nlm.nih.gov/geo/) under the accession number GSE43638.

SUPPLEMENTAL INFORMATION

Supplemental Information includes six figures, eight tables, and Supplemental Experimental Procedures and can be found with this article online at http://dx.doi.org/10.1016/j.cmet.2013.03.003.

ACKNOWLEDGMENTS

The authors are grateful to Dr. Fafournoux (INRA de Theix, France) for the gift of amino-acid-starved media. We thank Dr. Kwiatkowski (Harvard Medical School, Boston, MA) for the gift of $TSC2^{-/-}$ MEFs. We thank Dr. D. Avizonis for metabolomic analyses, C. Ouellet for mouse husbandry, M. Caron for bioinformatics analyses, T. Alain and M. Ghahremani for technical assistance, and D.W.K. Tsang, B.D. Fonseca, and G. Deblois for helpful discussions. This work was supported by grants from the Canadian Foundation for Innovation, the Canadian Institutes for Health Research (MOP-84227, MOP-111144), and a Program Project Grant from the Terry Fox Foundation (TFF-116128) to V.G. and N.S.

Received: August 7, 2012
Revised: November 16, 2012
Accepted: March 6, 2013
Published: April 2, 2013

REFERENCES

Bachmann, R.A., Kim, J.H., Wu, A.L., Park, I.H., and Chen, J. (2006). A nuclear transport signal in mammalian target of rapamycin is critical for its cytoplasmic signaling to S6 kinase 1. J. Biol. Chem. *281*, 7357–7363.

Blanchard, P.G., Festuccia, W.T., Houde, V.P., St-Pierre, P., Brûlé, S., Turcotte, V., Côté, M., Bellmann, K., Marette, A., and Deshaies, Y. (2012). Major involvement of mTOR in the PPARγ-induced stimulation of adipose tissue lipid uptake and fat accretion. J. Lipid Res. *53*, 1117–1125.

Blättler, S.M., Cunningham, J.T., Verdeguer, F., Chim, H., Haas, W., Liu, H., Romanino, K., Rüegg, M.A., Gygi, S.P., Shi, Y., and Puigserver, P. (2012). Yin Yang 1 deficiency in skeletal muscle protects against rapamycin-induced diabetic-like symptoms through activation of insulin/IGF signaling. Cell Metab. *15*, 505–517.

Carrière, L., Graziani, S., Alibert, O., Ghavi-Helm, Y., Boussouar, F., Humbertclaude, H., Jounier, S., Aude, J.C., Keime, C., Murvai, J., et al. (2012). Genomic binding of Pol III transcription machinery and relationship with TFIIS transcription factor distribution in mouse embryonic stem cells. Nucleic Acids Res. *40*, 270–283.

Charest-Marcotte, A., Dufour, C.R., Wilson, B.J., Tremblay, A.M., Eichner, L.J., Arlow, D.H., Mootha, V.K., and Giguère, V. (2010). The homeobox protein Prox1 is a negative modulator of ERRα/PGC-1α bioenergetic functions. Genes Dev. *24*, 537–542.

Chotechuang, N., Azzout-Marniche, D., Bos, C., Chaumontet, C., Gaudichon, C., and Tomé, D. (2011). Down-regulation of the ubiquitin-proteasome proteolysis system by amino acids and insulin involves the adenosine monophosphate-activated protein kinase and mammalian target of rapamycin pathways in rat hepatocytes. Amino Acids *41*, 457–468.

Cohen, P., Miyazaki, M., Socci, N.D., Hagge-Greenberg, A., Liedtke, W., Soukas, A.A., Sharma, R., Hudgins, L.C., Ntambi, J.M., and Friedman, J.M. (2002). Role for stearoyl-CoA desaturase-1 in leptin-mediated weight loss. Science *297*, 240–243.

Cunningham, J.T., Rodgers, J.T., Arlow, D.H., Vazquez, F., Mootha, V.K., and Puigserver, P. (2007). mTOR controls mitochondrial oxidative function through a YY1-PGC-1α transcriptional complex. Nature *450*, 736–740.

Deblois, G., and Giguère, V. (2011). Functional and physiological genomics of estrogen-related receptors (ERRs) in health and disease. Biochim. Biophys. Acta *1812*, 1032–1040.

Dufour, C.R., Levasseur, M.-P., Pham, N.H.H., Eichner, L.J., Wilson, B.J., Charest-Marcotte, A., Duguay, D., Poirier-Héon, J.-F., Cermakian, N., and Giguère, V. (2011). Genomic convergence among ERRα, PROX1, and BMAL1 in the control of metabolic clock outputs. PLoS Genet. *7*, e1002143.

Eichner, L.J., and Giguère, V. (2011). Estrogen related receptors (ERRs): a new dawn in transcriptional control of mitochondrial gene networks. Mitochondrion *11*, 544–552.

García-Morales, P., Hernando, E., Carrasco-García, E., Menéndez-Gutierrez, M.P., Saceda, M., and Martínez-Lacaci, I. (2006). Cyclin D3 is down-regulated by rapamycin in HER-2-overexpressing breast cancer cells. Mol. Cancer Ther. *5*, 2172–2181.

Giguère, V. (2008). Transcriptional control of energy homeostasis by the estrogen-related receptors. Endocr. Rev. *29*, 677–696.

Gulati, P., and Thomas, G. (2007). Nutrient sensing in the mTOR/S6K1 signalling pathway. Biochem. Soc. Trans. *35*, 236–238.

Gulati, P., Gaspers, L.D., Dann, S.G., Joaquin, M., Nobukuni, T., Natt, F., Kozma, S.C., Thomas, A.P., and Thomas, G. (2008). Amino acids activate mTOR complex 1 via Ca2+/CaM signaling to hVps34. Cell Metab. *7*, 456–465.

Handschin, C., and Mootha, V.K. (2005). Estrogen-related receptor α (ERRα): A novel target in type 2 diabetes. Drug Discov. Today Ther. Strateg. *2*, 151–156.

Harston, R.K., McKillop, J.C., Moschella, P.C., Van Laer, A., Quinones, L.S., Baicu, C.F., Balasubramanian, S., Zile, M.R., and Kuppuswamy, D. (2011). Rapamycin treatment augments both protein ubiquitination and Akt activation in pressure-overloaded rat myocardium. Am. J. Physiol. Heart Circ. Physiol. *300*, H1696–H1706.

Houde, V.P., Brûlé, S., Festuccia, W.T., Blanchard, P.G., Bellmann, K., Deshaies, Y., and Marette, A. (2010). Chronic rapamycin treatment causes glucose intolerance and hyperlipidemia by upregulating hepatic gluconeogenesis and impairing lipid deposition in adipose tissue. Diabetes *59*, 1338–1348.

Inoki, K., Kim, J., and Guan, K.L. (2012). AMPK and mTOR in cellular energy homeostasis and drug targets. Annu. Rev. Pharmacol. Toxicol. *52*, 381–400.

Jin, H.K., Ahn, S.H., Yoon, J.W., Park, J.W., Lee, E.K., Yoo, J.S., Lee, J.C., Choi, W.S., and Han, J.W. (2009). Rapamycin down-regulates inducible nitric oxide synthase by inducing proteasomal degradation. Biol. Pharm. Bull. *32*, 988–992.

Kantidakis, T., Ramsbottom, B.A., Birch, J.L., Dowding, S.N., and White, R.J. (2010). mTOR associates with TFIIIC, is found at tRNA and 5S rRNA genes, and targets their repressor Maf1. Proc. Natl. Acad. Sci. USA *107*, 11823–11828.

Kim, J.E., and Chen, J. (2000). Cytoplasmic-nuclear shuttling of FKBP12-rapamycin-associated protein is involved in rapamycin-sensitive signaling and translation initiation. Proc. Natl. Acad. Sci. USA *97*, 14340–14345.

Kim, J., Kundu, M., Viollet, B., and Guan, K.L. (2011). AMPK and mTOR regulate autophagy through direct phosphorylation of Ulk1. Nat. Cell Biol. *13*, 132–141.

Levy, G., Schmidli, H., Punch, J., Tuttle-Newhall, E., Mayer, D., Neuhaus, P., Samuel, D., Nashan, B., Klempnauer, J., Langnas, A., et al. (2006). Safety, tolerability, and efficacy of everolimus in de novo liver transplant recipients: 12- and 36-month results. Liver Transpl. *12*, 1640–1648.

Li, H., Tsang, C.K., Watkins, M., Bertram, P.G., and Zheng, X.F. (2006). Nutrient regulates Tor1 nuclear localization and association with rDNA promoter. Nature *442*, 1058–1061.

Luo, J., Sladek, R., Carrier, J., Bader, J.-A., Richard, D., and Giguère, V. (2003). Reduced fat mass in mice lacking orphan nuclear receptor estrogen-related receptor α. Mol. Cell. Biol. *23*, 7947–7956.

Morrisett, J.D., Abdel-Fattah, G., Hoogeveen, R., Mitchell, E., Ballantyne, C.M., Pownall, H.J., Opekun, A.R., Jaffe, J.S., Oppermann, S., and Kahan, B.D. (2002). Effects of sirolimus on plasma lipids, lipoprotein levels, and fatty acid metabolism in renal transplant patients. J. Lipid Res. *43*, 1170–1180.

Patch, R.J., Searle, L.L., Kim, A.J., De, D., Zhu, X., Askari, H.B., O'Neill, J.C., Abad, M.C., Rentzeperis, D., Liu, J., et al. (2011). Identification of diaryl ether-based ligands for estrogen-related receptor α as potential antidiabetic agents. J. Med. Chem. *54*, 788–808.

Patsenker, E., Schneider, V., Ledermann, M., Saegesser, H., Dorn, C., Hellerbrand, C., and Stickel, F. (2011). Potent antifibrotic activity of mTOR inhibitors sirolimus and everolimus but not of cyclosporine A and tacrolimus in experimental liver fibrosis. J. Hepatol. *55*, 388–398.

Peng, T., Golub, T.R., and Sabatini, D.M. (2002). The immunosuppressant rapamycin mimics a starvation-like signal distinct from amino acid and glucose deprivation. Mol. Cell. Biol. *22*, 5575–5584.

Peterson, T.R., Sengupta, S.S., Harris, T.E., Carmack, A.E., Kang, S.A., Balderas, E., Guertin, D.A., Madden, K.L., Carpenter, A.E., Finck, B.N., and Sabatini, D.M. (2011). mTOR complex 1 regulates lipin 1 localization to control the SREBP pathway. Cell *146*, 408–420.

Porstmann, T., Santos, C.R., Griffiths, B., Cully, M., Wu, M., Leevers, S., Griffiths, J.R., Chung, Y.L., and Schulze, A. (2008). SREBP activity is regulated by mTORC1 and contributes to Akt-dependent cell growth. Cell Metab. *8*, 224–236.

Risson, V., Mazelin, L., Roceri, M., Sanchez, H., Moncollin, V., Corneloup, C., Richard-Bulteau, H., Vignaud, A., Baas, D., Defour, A., et al. (2009). Muscle inactivation of mTOR causes metabolic and dystrophin defects leading to severe myopathy. J. Cell Biol. *187*, 859–874.

Rosner, M., and Hengstschläger, M. (2008). Cytoplasmic and nuclear distribution of the protein complexes mTORC1 and mTORC2: rapamycin triggers dephosphorylation and delocalization of the mTORC2 components rictor and sin1. Hum. Mol. Genet. *17*, 2934–2948.

Sarbassov, D.D., Ali, S.M., Sengupta, S., Sheen, J.H., Hsu, P.P., Bagley, A.F., Markhard, A.L., and Sabatini, D.M. (2006). Prolonged rapamycin treatment inhibits mTORC2 assembly and Akt/PKB. Mol. Cell *22*, 159–168.

Shor, B., Wu, J., Shakey, Q., Toral-Barza, L., Shi, C., Follettie, M., and Yu, K. (2010). Requirement of the mTOR kinase for the regulation of Maf1 phosphorylation and control of RNA polymerase III-dependent transcription in cancer cells. J. Biol. Chem. *285*, 15380–15392.

Sladek, R., Bader, J.-A., and Giguère, V. (1997). The orphan nuclear receptor estrogen-related receptor α is a transcriptional regulator of the human medium-chain acyl coenzyme A dehydrogenase gene. Mol. Cell. Biol. *17*, 5400–5409.

Sonenberg, N., and Hinnebusch, A.G. (2009). Regulation of translation initiation in eukaryotes: mechanisms and biological targets. Cell *136*, 731–745.

Tsang, C.K., Liu, H., and Zheng, X.F. (2010). mTOR binds to the promoters of RNA polymerase I- and III-transcribed genes. Cell Cycle *9*, 953–957.

Vega, R.B., and Kelly, D.P. (1997). A role for estrogen-related receptor α in the control of mitochondrial fatty acid β-oxidation during brown adipocyte differentiation. J. Biol. Chem. *272*, 31693–31699.

Villena, J.A., and Kralli, A. (2008). ERRalpha: a metabolic function for the oldest orphan. Trends Endocrinol. Metab. *19*, 269–276.

Wullschleger, S., Loewith, R., and Hall, M.N. (2006). TOR signaling in growth and metabolism. Cell *124*, 471–484.

Yamauchi, Y., Furukawa, K., Hamamura, K., and Furukawa, K. (2011). Positive feedback loop between PI3K-Akt-mTORC1 signaling and the lipogenic pathway boosts Akt signaling: induction of the lipogenic pathway by a melanoma antigen. Cancer Res. *71*, 4989–4997.

Yang, S.B., Lee, H.Y., Young, D.M., Tien, A.C., Rowson-Baldwin, A., Shu, Y.Y., Jan, Y.N., and Jan, L.Y. (2012). Rapamycin induces glucose intolerance in mice by reducing islet mass, insulin content, and insulin sensitivity. J. Mol. Med. *90*, 575–585.

Yu, L., McPhee, C.K., Zheng, L., Mardones, G.A., Rong, Y., Peng, J., Mi, N., Zhao, Y., Liu, Z., Wan, F., et al. (2010). Termination of autophagy and reformation of lysosomes regulated by mTOR. Nature *465*, 942–946.

Zhang, X., Shu, L., Hosoi, H., Murti, K.G., and Houghton, P.J. (2002). Predominant nuclear localization of mammalian target of rapamycin in normal and malignant cells in culture. J. Biol. Chem. *277*, 28127–28134.